CHAPTER 1

INTRODUCTION AND LITERATURE REVIEW

1.1 INTRODUCTION

The stringent demand for energy has accelerated the advancement in technology for power plants and other energy generation units. Consequently, close monitoring is required for each individual components and assemblies for their efficient utilization and output. Each of these components is operated in the temperature range of 200-800°C. When exposed to such high temperatures, the metallic substrate suffers hot-corrosion and development of thick scales (oxides, sulfides, etc.) leading to the synergistic interaction between solid particle erosion (SPE) and corrosion. Erosion-corrosion is of considerable technical importance in several applications including coal gasification, steam turbines,

Fig. 1.1: Components suffering from material degradation due to erosion-corrosion.

gas turbines, water walls, and heat exchanger tubes (Fig. 1.1). Among the various components of power plants, heat exchangers play the most critical role in improving the efficiency of the plant.

Erosion is a wear process that occurs due to mechanical interaction between particles and the surface when discrete solid particles strike a surface causing the removal of materials. The contribution of target material properties is significant in the surface degradation mechanism, though the erosion takes place when the hardness of impacting particles are more than the target material. Amidst several most influencing parameters, the erosion rate of material under high-temperature conditions is not much excavated and thus needs close examination. High-temperature erosion wear is a crucial problem in the coal-burning electricity generation industry, which often suffers the direct and indirect loss due to the maintenance of the unit. Therefore, continuous research for better material is crucial in this endeavor.

1.2 SOLID PARTICLE EROSION

Solid particle erosion (SPE) is a wear process in which loss of material results from the surface by the impact of tiny solid particles causing highly localized stresses. Erosion resulting from solid particle impact is a problem of considerable practical significance, which can result in component failure in, for example, heat exchanger tubes, turbines, and other energy conversion systems. At the same time, it should be recognized that erosion has some beneficial aspects, for example, sandblasting, abrasive water jet machining, shot peening, ultrasonic cleaning, etc.

Thinning of component, macroscopic scooping appearance, surface roughening and formation of ripple pattern of few of the metals are some usual manifestations of

SPE. Solid particle erosion refers to a stream of particles striking and rebounding from the surface. The contact force exerted by the surface decelerates the particles. The loss of materials is defined in terms of erosion rate (E), as the ratio of the mass of material removed per unit mass of erodent impact. E is dependent on power-law velocity which is expressed as:

$$E = kV^n \tag{1.1}$$

where,

k = constant

V= impact velocity

n = velocity exponent (3 to 3.5 for metals).

1.3 HISTORICAL SIGNIFICANCE

Erosion is derived from the Latin word 'rodere' means to 'gnaw'. The study of erosion has long history and starts with some popular names like Reynolds [1] who wrote a paper on sandblasting in 1873. Lord Rayleigh [2] addressed this topic in 1912. Famous Brooklyn Bridge construction in 1870 marked the witness of erosion in human history for the first time. However, the study for the basic mechanism involved in erosion started post World War-II. In 1980, the American military mission, where erosion of turbine blades contributed to the failure of the mission, was hailed as an act of God.

In erosion literature, based on the dependence of erosion rate on impact angle, materials are broadly classified as ductile or brittle. Wellinger et al. [3] studied the effect of impact angle (α) on the erosion of both soft and hard materials, and found the weight loss W, to be greater for ductile/soft materials at $\alpha \rightarrow 0°$ and as $\alpha \rightarrow 90°$ erosion rate maximized for brittle/hard materials. This dependence on weight loss for ductile and

brittle materials has been further excavated and has been procreated on a number of occasions [4–6]**.** The ductile materials like metals and alloys exhibit a maximum erosion rate at oblique impact i.e. 15° to 30°. In contrast, the maximum erosion rate of a brittle material is obtained at a normal impact (i.e. 90°) (Fig. 1.2).

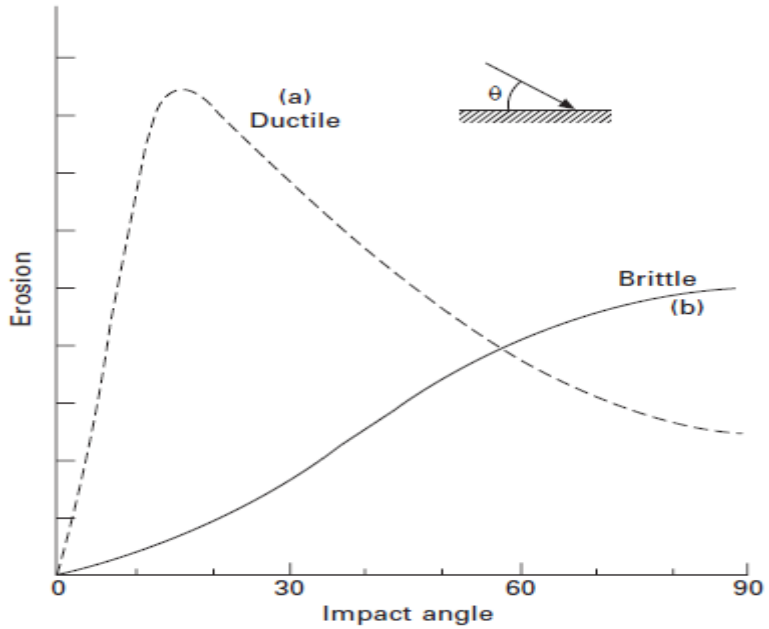

Fig. 1.2: Typical dependence of erosion on impact angle for ductile materials (curve a) and brittle materials (curve b) [7]**.**

1.4 MECHANISM OF EROSION

The erosion scars generated over the surface explains the behavior of multiple particles impacting on the surface. The erosion mechanism is seen to vary depending upon the materials property, where ductile metals usually involve plastic flow, while brittle materials wear predominantly by fracture.

1.4.1 Ductile Materials

Weight loss from the surface of ductile material occurs by the virtue of various physical properties, of which plastic deformation is most influential. At a low grazing angle, the particle strikes and leaves the surface forming a crater, while at intermediate

impact, removal of chip takes place by cutting. At higher impact angles, materials are piled at the end of craters, which is removed by subsequent impacts. Hutching et al. [8] studied the plastic deformation behavior on a ductile metal. Ploughing occurs at 30° impingement of spherical particles, that displaces materials to sides. The angular particles deform the materials on the basis of its orientation of impact. Type –I cutting mode occurs when particle rolls forward indenting the surface and raising materials into a pronounced lip. The reverse rotation of these angular particles causes Type-II cutting, which occurs over only a limited array of particle geometries and impact orientation (Fig. 1.3). The detachment of plastic rupture of metal as wear debris takes place only after experiencing several cycles of plastic deformation and becoming severely work hardened. Finnie et al. [9] neglected the effect of particle rotation. Later, Deng et al. [10] deemed particle dynamics effect on erosion test conditions. They found that air drag force acts as the main accelerating force and the particles are influenced by turbulence and particle collisions. The turbulent atmosphere causes the suspended particles to rotate about their own center. Since the particles are angular, the rotational component may cause additional damage to the surface. However, in the experiment conducted by Deng et.al this rotational factor has very limited influence. Not all the particles leaving the nozzle are responsible for causing erosion. Hutchings et al. [11] observed only 1/6 of the particles **(**at $\alpha = 20°$), removed a chip without leaving materials piled up on the eroded surface. Gane and Murray [12] approximated this fraction to be ½.

Beyond the maximum erosion angle, particles come to rest on the surface while cutting materials gets piled up ahead of the particles. The volume removed is equal to the volume swept out of the tip of particles. At higher angles, the removal of the materials is assigned several mechanisms like work hardening, fragmentation of particles, low cycle

fatigue, temperature effects due to strain rate and delamination wear. Figure 1.4 shows the schematic for erosion procedure in a ductile material. Mayville [13] intended a mechanism of platelet formation accompanied by cutting for normal impacts.

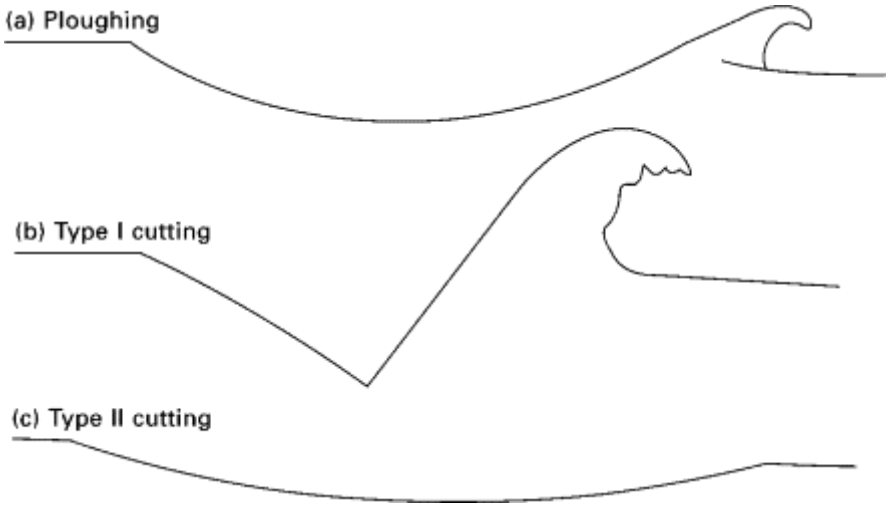

Fig. 1.3: Cutting Mechanism during oblique impact erosion [7].

Annealed FCC metals and numerous other annealed metals show a volume removal that is inversely proportional to hardness. Steels having an inferior rate of strain hardening than annealed FCC metals show a much higher erosion rate. The heat treatment process causing an increase in VHN is virtually ineffective to erosion. In addition, as the hardness of the steel increases, the angle dependence shows brittle behavior for ductile materials. Prior cold working although increases the hardness but doesn't affect erosion because the flow stress at large strain should change very little due to prior deformation.

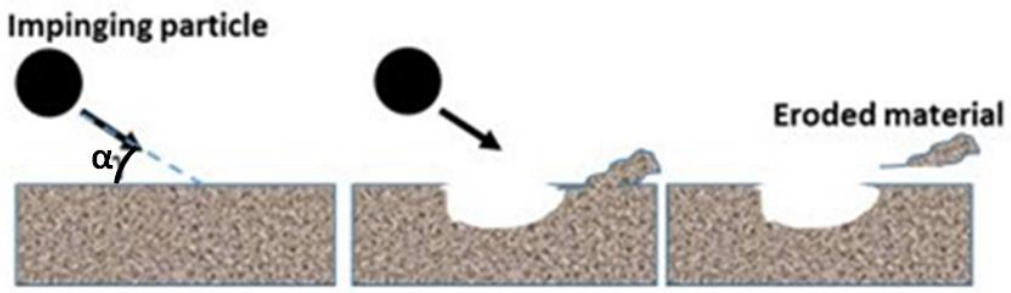

Fig. 1.4: Schematic of erosion procedure in ductile material [14].

1.4.2 Brittle Materials

In such materials, erosion contemporizes by propagation and intersection of cracks, created by impacting particles (Fig. 1.5). Failure of brittle material is based on Hertz theory, which states that Hertzian cone crack is based on three stresses:

I. Maximum tensile stress acts on the surface at the fringe of the contact circle.
II. Maximum compressive stress acts normal to the target surface at the center of the circle of contact.
III. Maximum shear stress at a depth of approximately half of the contact radius, directly below the center of the contact circle.

The cone is initiated from the flaw at the surface and at the fringe of the circle of contact, having radius typically few percents larger than the contact radius. Creating an intersection of cracks forms a chip and loosen it from the surface. Thus, chip formation depends not only on the number of particles striking and the force rather on the distribution of flaws in that surface. Finnie [15] stated that with the reduced particle size, brittle material starts to erode in symptomatically ductile manner. This is because, with the decrease in particle size, the effective stressed volume decreases and so the possibility of containing a critical flaw also decreases. Therefore, the fracture strength of the brittle solid increases. In such a situation, flow occurs before fracture. The crystal structure also plays an important role in determining the erosion resistance of a metal. The erosivity of BCC metals is typically two to three times faster than do FCC metals of similar hardness.

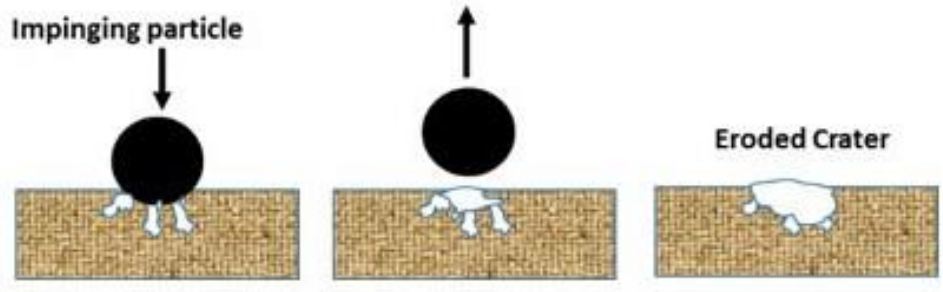

Fig. 1.5: Schematic of erosion procedure in brittle material [14].

1.5 EROSION MODEL

It is broadly agreed that metal removal occurs due to extensive plastic shear, however, the model of steady-state erosion to explain the critical property of the materials causing erosion is a must. Several models are facilitated by researchers, on the basis of different modes of erosion.

1.5.1 Cutting Models

Finnie [16] expressed that erosion on the surface of a material struck by solid particle counts on the motion of the particle and target properties. Erosion in the ductile materials begins with plastic deformation and in brittle materials by the intersection of cracks. He proposed the following equation:

$$\varepsilon_{vp} = \frac{m_p V_p^{\,2}}{P\psi k}\left[\frac{k\cos 2\alpha}{6}\right] \qquad \text{for } \tan\alpha \geq k/6 \qquad (1.2)$$

$$\varepsilon_{vp} = \frac{m_p V_p^{\,2}}{P\psi k}\left[\sin(2\alpha) - \frac{6}{k}\sin^2\alpha\right] \qquad \text{for } \tan\alpha \leq k/6 \qquad (1.3)$$

Bitter [17] stated repeated deformation and cutting are two mechanisms for erosion. Based on energy balance for a plastic-elastic collision, the erosion induced by the deformation mechanism is predicted using the following equation:

$$\varepsilon_{vp} = \frac{1}{2}\frac{M(\mathrm{V_p}\sin\alpha - k)^2}{\delta} \tag{1.4}$$

1.5.2 Localization Models

Sundararajan and Shewmon [18] suggested a model that considers the shear localization leading to lip formation as a function of critical strain as mentioned in equation below:

$$\varepsilon_m = \frac{6.5X10^{-3}V_p^{\,2.5}\rho_p^{\,2.5}}{C_p T_m^{\,0.75} H_t^{\,0.25}} \tag{1.5}$$

Reddy and Sundararajan [19] conducted experiments using a constant velocity of 40 m/s at impact angles of 30°, 60°, and 90° on two ductile materials. Based on the SEM micrograph, they suggested that lip formation and fracture are the fundamental erosion mechanisms. They showed that the erosion rate corresponds to the following relation:

$$\varepsilon_{vp}\alpha\frac{L^3\Delta\Omega_m}{\Omega_c} \tag{1.6}$$

Granados et al. [20] analyzed the effect of swirling jet erosion on AISI-310SS at 450°C tested under 30°, 60°, and 90° impact. Swirling jet is defined as axisymmetric flow with rotation. The results show that erosive wear rates increase with the increase in temperature. Plastic deformation, crack formation and ploughing are the predominant mechanisms. But erosion tendency under swirling as well as non-swirling conditions was similar.

1.5.3 Delamination Model

Jahanmir [21] developed a model in which inclusions become the epicenter for voids nucleation beneath the impact surface. The depth of formation of these voids

increases with impact velocity as they grow into subsurface microcracks. This leads to material removal in the form of thin laminae.

1.5.4 Fatigue Model

Based on low cycle fatigue theory, at normal impacts, it is assumed that an element of volume will be lost once it acquires a critical strain. Hutchings [22] model predicted that the erosion rate will be inversely related to the product of the target yield strength and its fracture strain. The velocity exponent (n) of the model was predicted as 3. While at oblique impacts, Ratner and Stytter [23] equated volume undergoing heavy deformation with the volume of the crater. The model predicted a velocity exponent of 3.5. Evstifeev et al. [24] studied the SPE of a compressor blade steel (EI-961 grade) on the basis of the incubation time concept. They regarded erosion-based damage as a dynamic process. Thus, dynamic fracture involving time-based strength parameter i.e. incubation time, developed into a common criterion to predict threshold velocities of the surface damage process.

1.5.5 Adiabatic Shear Induced Spalling Model

The removal of chunks of the target material is the result of intersecting shear bands formation in the crippled volume beneath the crater. The formation of adiabatic shear bands requires a critical strain and deformation. Therefore, their formation is obvious in high strength alloy. If this mechanism prevails, the angle of maximum weight loss will appear at higher angles than for those metals where shear is more homogeneous.

1.6 PARAMETERS INFLUENCING SOLID PARTICLE EROSION

Erosion is seen to be influenced by several parameters like erodent properties, target material properties, fluid properties, impact conditions, and temperature effect.

Particle properties have a significant repercussion on SPE. The effect of each factor like size, density, shape, and hardness have been investigated by researchers separately. Some of them are discussed below:

1.6.1 Particle Shape

Particle shape has a radical significance on the magnitude of erosion. Researchers in the past [25,26] conducted an experiment and found that erosion resulting from angular particles was four times higher compared to erosion result from spherical particles. Hutchings et al. [27] introduced a 'particle shape factor' in the erosion rate equation to cater to the erosion magnitude. Lin et al. [28] examined the influence of particle size, shape and flux rate on the erosion of 316SS. They observed that erosion rate is radically affected by particle shape than particle size. Torres et al. [29] investigated the performance of AISI 420SS. The angular silicon carbides and steel round grit of 60 mesh was used. It was observed that higher mass loss occurs by angular particle impact. The erosion rate was maximum at 30° and decreased with an increase in impact angle.

1.6.2 Particle Size

The kinetic energy associated with a larger particle is high and so, is the erosion rate. On the other hand, smaller sand particles are more affected by turbulence. This leads to an exchange in momentum between fluid particles. Tilly [6], stated that erosion is nearly independent of particle size if it exceeds 100 µm. Particle size and erosion rate exhibit linear relation, as observed by other researchers [30–32]. Desale et al. [33] studied the erosion performance on aluminium alloys using silica sand size between 3.5-655 µm and concluded that erosion rate increases with particle size for a constant flux. They recommended a correlation for erosion rate as:

$$\text{Erosion Rate } \alpha \text{ (Particle Size)}^n$$

Nguyen et al. [34] extended their study to the sand particle size effect. It is observed that smaller sized particles create a larger diameter of the erosion pattern. But when erosion rate is concerned it is observed that the erosion rate increases as the particle size increases. And reaches a maximum value at 150 μm particle size.

1.6.3 Particle Material

Density and hardness are key properties of the particles responsible for erosion. Denser particles will have higher kinetic energy and create more impact force causing enhanced erosion rate. Levy and Chik [25] examined the effect of particle hardness on erosion behavior of AISI 1020 carbon steel. The behavior of three erodents showed that the erodent with higher hardness causes slightly more erosion. Although there exists an interrelationship between the hardness of target material, the hardness of particle and erosion rate. Wada et al. [35] suggested this correlation as

$$\text{Erosion Rate } \alpha \ (\frac{H_t}{H_p})^n$$

Shipway and Hutchings [36] recorded a steep increase in erosion rate and reduction in velocity exponent as the ratio of erodent to target hardness tends towards unity. It is also stated that the erosion rate is autonomous to particle hardness greater than 700 HV. Arabnejad et al. [37] studied the impression of particle hardness on the erosion of stainless steel at low impingement velocity. Erosion rate increases with increasing hardness of the particle as long as the target material is harder than the particle.

1.6.4 Sand Concentration

Several mechanisms have been proposed that explain the relationship between erosion rate and sand concentration [38,39]**.** At high sand flux, rebounding off the particles from the surface retards the further incoming particle. This phenomenon is

called 'Shielding' [10,40]**.** Therefore, the higher sand concentration may result in a lower erosion rate.

1.6.5 Impact Velocity

The erosion rate being directly proportional to impact velocity (V^n), various researchers have suggested the values of 'n', typically varying from 1.6 to 2.6 [41–43]. Parsi et al. [44] observed through CFD simulation that the final erosion rate is influenced by surface deformation during the erosion process. They found that the erosion rate decreased as the surface of the specimen became deeper by particle impact. Saarivirta et al. [45] conducted a test on different boiler steels with three different erodents at low impact velocity. Grade P265GH showed the highest wear coefficient K, suggesting the greatest loss by the impact. The sand erodent brought evident wear damage in steels but ash as erodent was not effective. This low damage rates in erosion were due to the agglomeration tendency in the ash. Okonkwo et al. [46] investigated the erosion behavior mechanism for API X-42 pipeline steel keeping impingement angle constant. The results showed that low-velocity impingement has plastic deformation, embedment of erodent particle on the surface and ploughing as the erosion mechanism, whereas, higher velocity subjected to longer test duration suffers erosion mainly by ploughing.

1.6.6 Impact Angle

The influence of the impingement angle on erosion varies on the basis of the materials surface. For ductile materials, higher erosion rate occurs at oblique impact, due to adequate formation and cutting of platelets by particles at oblique angles. On the contrary, brittle materials undergo maximum erosion at the normal impingement angle as a result of cracking. Nguyen et al. [47] investigated the effect of erosion on 304SS and revealed two different erosion regime. Plastic deformation dominates at high impact

angles while ploughing/cutting mechanism dominates at low impact angles. In addition, for a fixed incident angle, the erosion rate was seen to be proportionate to impact velocity. Zdravecka et al. [48] used SiO_2 sand particles at 50 m/s for 15°,45°, and 90°. At 15°, ductile wear with cutting and ploughing dominated, while at 90°, apart from grooving effect the deformation mechanism of wear co-exists.

1.6.7 Target Material Properties

No clear correlation between target materials and SPE is made. But, it has been admitted that higher material hardness caused reduced erosion rate [15]. This was contradicted by Levy and Hickey [49]**,** on the basis of ductility, which distributed the kinetic energy of an impact by plastic deformation culminating in lower erosion rate. Toughness demonstrates a better erosion performance where the hardness is reduced without reducing the ductility. Chauhan et al. [50] studied the SPE of 21-4-N and 13/4 steel. They found that erosion resistance offered by 13/4 is comparatively low to that offered by 21-4-N. Hot rolling of 21-4-N improved the erosion property. This is due to the austenitic matrix of 21-4-N which likely offers more resistance to erosion damage. Singh et al. [51] performed laser cladding on 13Cr-4Ni stainless steel to study erosion performance. It was found that cladding at 32 J/mm^2 showed significant resistance to SPE. This erosion resistance is illustrated on the grounds of dimensionless parameters related to kinetic energy. Kumar et al. [52] studied the response of heat treatment on erosion behavior of cast 23-8-N steel. The dissolution of carbides and the formation of equiaxed grains at 1220℃ resulted in the enhancement of erosion resistance. Mukhopadhyay et al. [53] explored the microstructural development of steels during solid particle erosion of 5100 and M50 steel. Disintegrated lath boundary, low angle grain boundaries, and shear bands are developed as impacted by solid particles. Oblique erosion is seen to induce greater breakage tendency. Normal erosion induces dynamic

recovery and microstructural heterogeneities. Laguna-Camacho [54] evaluated the performance of AISI 304, 316, and 420 SS to the erosion process. The materials were tested at low velocity with 150 g/min flow rate impacted at 30°, 60°, and 90°. Plastic deformation distinguished by pitting and cutting action was seen for 420SS and showed higher erosion damage at 30°. While 304 and 316 SS showed wear damage much alike brittle fracture with the detachments of large fragments. They showed an increased erosion rate at 60°. Islam et al. [55] investigated the effect of microstructure on the erosion of AISI 1018 and AISI 1080 steel for variable impact velocity and impact angles. AISI 1018 exhibits better erosion resistance than AISI 1080 steel. Ploughing, metal cutting, and delamination are the controlling mechanisms. At a low impact angle, AISI 1018 steel exhibits more embedded particles resulting in better erosion. Secondary metal cutting is customarily observed at the initial stage of erosion, however, its contribution is meagre at high abrasives feed rate.

1.6.8 Temperature Effect

Several hypotheses of temperature dependence on erosion have been proposed. Levy et al. [56] state that an increase in temperature increases the ductility of the material, which helps in absorbing the kinetic energy of the impact, thereby, decreases the erosion rate. Figure 1.6 shows the temperature dependence of erosion that is categorized into three groups:

Ist group: initially the erosion rate decreases with increasing temperature, reaches the lowest and then increases with the increase in temperature.

IInd group: exhibits temperature-independent erosion rate up to a critical temperature followed by rising erosion rate.

IIIrd group: shows a consistent increasing erosion rate with temperature.

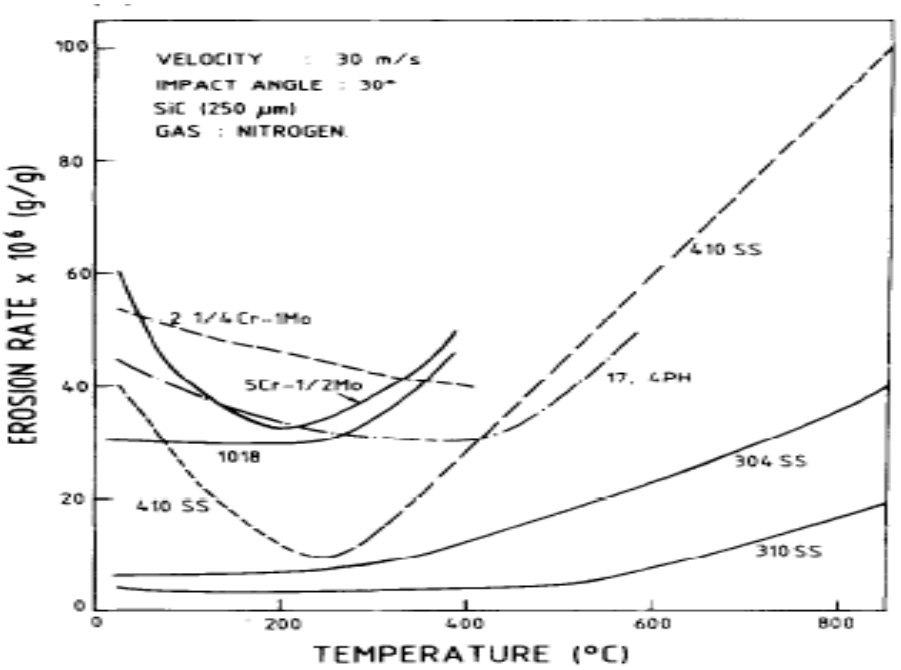

Fig. 1.6: Temperature dependent erosion rate for different steels [57].

The dependence of erosion on the impact angle at elevated temperature exhibits conflicting observations. Levy et al. [58] obtained higher erosion at a normal impact for 9Cr-1Mo Steel at 850℃ with 35-70 m/s impact velocity. Chang et al. [59] indicated peak erosion at 60° for cobalt when tested at 780℃ using 70-140 m/s impact velocity. With the reduction in temperature to 600℃, the erosion rate peaked at 30°. Wang et al. [60] conducted high-temperature solid particle erosion to identify the behavior of surface ripples and enduring erosion under angular particle impact. The results indicated large transverse ripples and small scale longitudinal ripples at 500-600℃. Under the continued intrusion of high-velocity particles, the surface morphology mutated from disordered scars to coherent ripples. Saarivirta et al. [61] conducted erosion tests of various fluidized bed boiler steels at elevated temperatures. The study concludes that there is an increment in oxidation rates for the steel with temperature. But, the oxidation rate is seen to decrease with an increase in chromium content. The low particle velocity causes ousting of particle

debris eventually causing weight gain, whereas, the highest velocity causes essential loss of material. The angle dependency of ductile erosion behavior changes with the increase in temperature. Shimizu et al. [62] studied the effect of mechanical properties on SPE of SUS403 and SUS630 stainless steel when subjected to 300,600 and 900°C. The impact velocity was 100 m/s with an impact angle of 30° and 90°. Deformation wear was the predominant mechanism for erosion at 90°. There existed a corresponding relationship between hardness and erosion rate. At 30° impact, the SUS403 stainless steel showed a double erosion rate than SUS630 stainless steel, suggesting that at a shallow impact, the protrusions are readily formed on the materials with higher elongation. These protrusions can be removed by further impacts. Antonov et al. [63] aimed to study the oxidation effect on erosive behavior of boiler steels at room temperature and elevated temperature. It is seen that oxidation enables improved resistance to erosion under the oblique angle of impact. A thin and soundly adhered layer of oxide is formed in the austenitic steels. These oxide films are capable of rehealing spontaneously and repeatedly. This property of austenitc steel makes it more vulnerable for erosion corrosion application where elevated temperature operation takes place in a cyclic mode.

The erosion test temperature for 304SS is seen to create an adverse effect on the velocity exponent decreasing to nearly 0.9. Levy et al. [57] studied the erosion rate for 9Cr-1Mo at 650°C and concluded that the velocity exponent initially remained steady for the initial period thereafter, increased with an increase in erodent size. Tabakoff and Vittal [64]**,** however, concluded that the erosion rate dependence on particle size is marginal and no significant effect of particle size is seen. Zhou and Bahadur [65] highlighted the concept of erosion rate independence on particle size beyond 40 μm. They also investigated the effect of erodent flux on the erosion of 304 and 430 SS over a

range of high temperatures. Their results indicated no change in erosion rate by increasing the flux rate at 500°C. However, beyond 500°C, a substantial higher erosion rate is seen with a slight increase in flux rate. The elevated temperature erosion at high impact velocity using angular particles was studied [66,67] and found metal erosion as the commanding regime under such conditions. The erosion resistance of ferritic steels is reasonably indicated by the strength of the material at elevated temperatures. Oxidation effect becomes more important for elevated temperature erosion tests carried out at low velocity and using spherical Al_2O_3. It is seen that high chromium content (exceeding 10-12%) terribly reduces the erosion rate. With steels having Cr ≤ 10%, thick Fe_2O_3 scales are formed which are likely to spall and consequently generate increased erosion rate. In contrast, steels with Cr ≥ 10% form segmented and thin Cr_2O_3 and spinel scales during erosion leading to low erosion rate. One such steel is Type 446 stainless steel with Cr ≥ 24%, which may possess high resistance to high-temperature erosion.

1.7 TYPE 446 STAINLESS STEEL

Stainless steel is a low maintenance material with large endurance. They have appreciable cost to life advantage over other grades of carbon steels. In the present scenario, 60% of newly developed stainless steels are recycled from melted scrap [68]**.** Apart from recyclability and low cost, these steels possess several appealing countenances like strong corrosion-resistance, creative appearance, heat resistance, biological neutrality, and uncomplicated fabrication. These characteristics of stainless steel are clearly displayed in Ferritic stainless steel which is a member of the stainless steel family. These steels contain higher chromium content ranging from 10.5 to 30 wt% and possess properties superior to austenitic steels on several occasions. The Fe–C–Cr diagram along 18% chromium, shown in Fig. 1.7, indicates that the austenite is not

possible to form until a very high temperature (1200 °C) is attained for the low carbon content of 0.06%. This leads to the fact that steel of this composition is ferritic from room temperature till 1200 °C and is not susceptible to hardening.

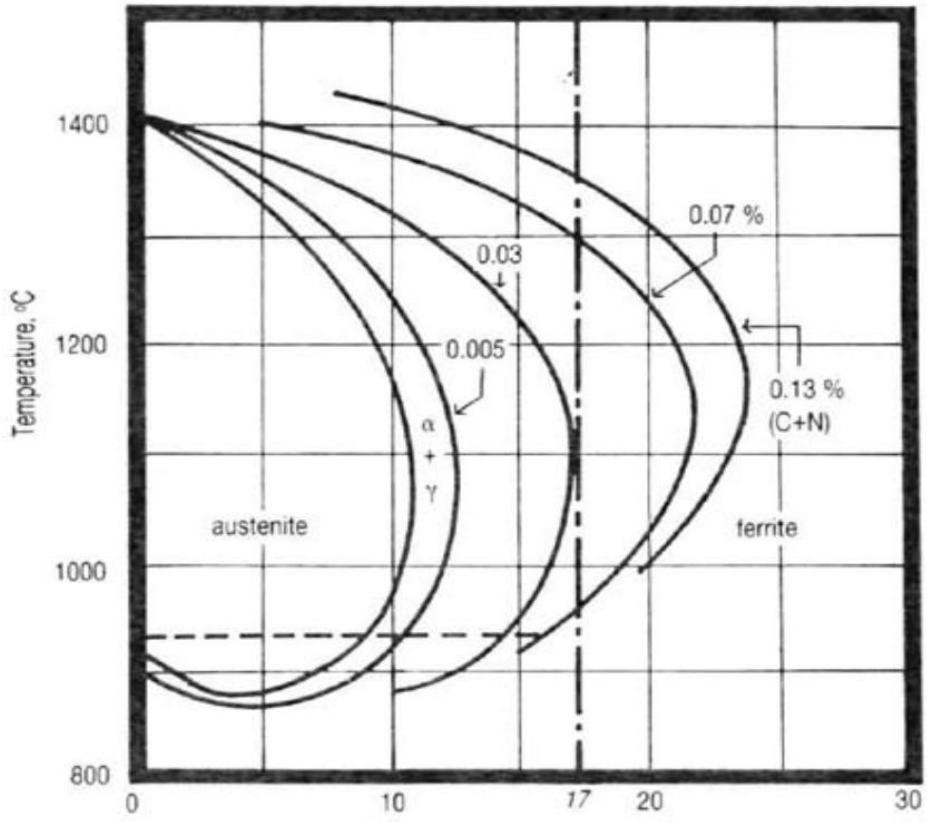

Fig. 1.7: Fe-Cr-C phase diagram [69].

Ferritic stainless steel is used in food industries and for architectural trims etc., as they are only responsive to cold working. The ferritic steels are extremely superior to low-carbon steels in annealed conditions. They are fairly stronger with soft and ductile character and carry good forming ability at the same time. Type 446 stainless steel has excellent oxidation resistance at elevated temperatures, high thermal conductivity, higher yield strength than austenitic stainless steels, and lower tensile ductility. In terms of corrosion resistance, these steels are preferable than martensitic stainless steel. Super ferritic steels such as Type 446 stainless steel is included in ASTM

specifications A176-74 (Chromium stainless flat products), A511 (Seamless stainless steel mechanical tubing), A268-74 (Ferritic stainless steel tubing for general service) and also in ASME code and AISI and SAE specifications. Type 446 stainless steel are high-chromium ferritic steels having 18-30% Cr and low content of carbon and nitrogen with excellent corrosion and oxidation resistance. This excellent resistance to general, intergranular and pitting corrosion and stress corrosion cracking is laid by the controlled composition and ferritic structure which makes it suitable for a wide variety of applications charged with chlorides, organic acids, and chloride stress-corrosion environment such as heat exchanger tubing, feed-water tubing and in equipment that operates with chloride-bearing or brackish cooling waters. Type 446 stainless steel serves the purpose with utmost adequacy and economy.

1.7.1 Structure and Constitution of Ferritic Stainless Steel

Ferritic stainless steel is chromium-rich (α) solid solution having a body-center-cubic crystal (BCC) structure with thinly dispersed carbide in the microstructure, at room temperature. Figure 1.8 shows the iron-chromium binary equilibrium phase diagram for ferritic stainless steel. These steels have magnetic property and have fewer slip systems, which lowers the plastic formability under plastic deformation.

Ferritic stainless steel is accessible in five different grades and acquires 25-40% of the total production of stainless steel. Some of these are classified as standard grades (Group 1, 2 and 3) and some as special grades (Group 4 and 5). Table 1.1 shows the classification of these steel grades. Lowest chromium content forms Group 1 while Group 2 with high chromium content is the most commonly used grade. They have high corrosion resistance and fulfill the purpose of replacing austenitic Grade 304.

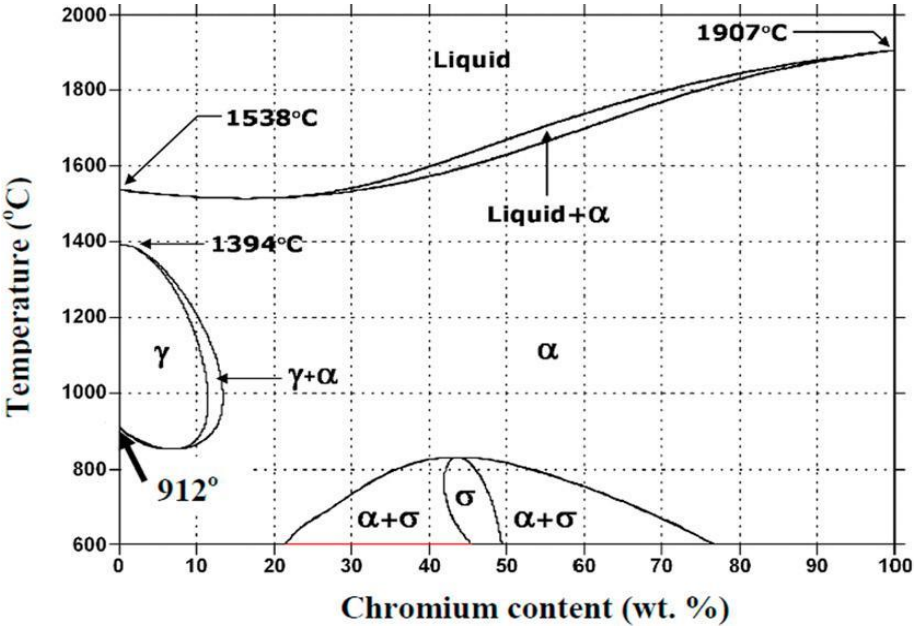

Fig. 1.8: Iron-chromium binary equilibrium phase diagram [70].

The Group 3 ferritic steel with chromium content up to 18 wt% has better welding and forming ability. The special grade ferritic steels of Group 4 has higher chromium with a higher Mo concentration of nearly 0.5wt%, while Group 5 has chromium in the range of 25-30wt% and Mo may increase up to 3wt%. This special grade ferritic steels with more than 20wt% chromium do not generally form austenite at any temperature and are called as "Superferritic grades".

1.7.2 Effects of Alloying Elements

The stability of ferritic stainless steel is largely dependent upon the ferrite and austenite phase stabilizing elements. The modified Schaffler's diagram (Fig.1.9) predicts the structure of stainless steel based on Ni and Cr equivalent. The general effect of alloying elements in ferritic steels are as follows:

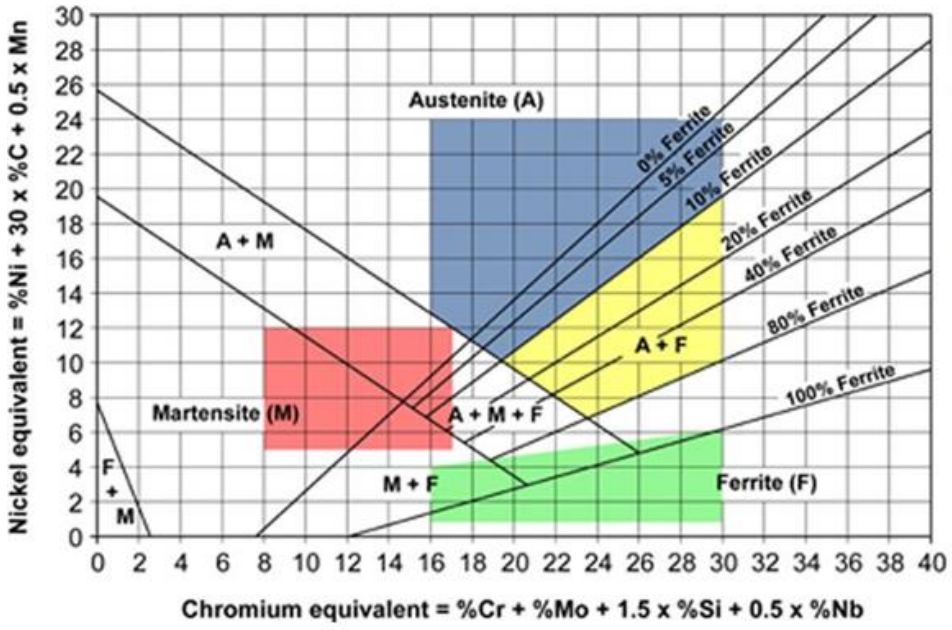

Fig. 1.9: Modified Schafflers diagram [71].

Table. 1.1: Classification of Ferritic stainless steel on the basis of chromium content and their market share [69].

Classification	Groups	Chromium wt%	Market share	Specific types
Standard ferritic grade	Group1	10-14	30 %	Type 409, 410, 420
	Group2	14-18	48 %	Type 430
	Group3	14-18 stabilized	13 %	Type 430 Ti, 441 with stabilizing elements like Ti, Mo etc.
Special ferritic grade	Group4	10-18 + 0.5% Mo	7 %	Type 434, 436, 444
	Group5	18-30	2 %	Type 445, 446, 447

Carbon: The majority of the carbon present appears as finely divided chromium carbide precipitates. The addition of carbon shows two effects on the phase diagram. Firstly, the narrow region of the two-phase field $\gamma + \alpha$ is expanded by shifting the austenite phase boundary towards higher chromium content. Also, this $\gamma + \alpha$ two-phase field is shifted to

a higher temperature. Secondly, the solubility of carbon being low in the α-matrix is rejected from a solid solution as complex carbides, which precipitates predominantly at the grain boundary. The Group 5 grade steel such as 446, 445 and 447, contains extra low carbon as interstitials to ensure sufficient structural stability.

Nitrogen: Nitrogen also acts as a powerful γ + α two-phase field expander. It complements the strength by forming an interstitial solid solution and retards the embrittlement by precipitation of sigma (σ) phase. Nitrogen occupies octahedral sites where lesser strain energy is required. The number of octahedral sites being low in the case of BCC structure, the solubility of nitrogen in ferritic steel is very low. Thus, extra nitrogen precipitates out to form Cr_2N which increases its resistance to localized corrosion.

Chromium: Chromium is a member of the group of ferrite phase stabilizers. It suppresses the gamma phase field and extends the sigma phase field. Beyond 13 wt% chromium, the transformation from α to γ is no longer possible. The superferritics having low interstitials and high chromium remains BCC throughout from room temperature to melting point and therefore, grain refinement and hardening by heat treatment and quenching are no longer possible.

Manganese: Similar to Cr, segregation of impurities at the grain boundaries is improved. It also replaces Ni to some extent and induces temper embrittlement. Manganese depresses the transformation from γ to α phase at lower temperatures.

Molybdenum: Improvement in pitting and crevice corrosion is achieved by Mo alloying. It is a distinct carbide former and ferrite phase stabilizer. Mo addition can produce fine-grained steels, improved fatigue strength, and delayed temper embrittlement. It also

improves nitrogen solubility on one hand but increases the sigma phase formation tendency too.

The Group 5 stainless steel has a chromium range of 25-30% and extremely sensitive to embrittlement due to precipitation of the intermetallic phase. Their uses are restricted to thin gauges as they are very difficult to weld. The high chromium and molybdenum containing grades are known as 'Superferritics'. These new generation grades of ferritic steel are designed to have an extra-low interstitial content, thereby, further diminishes the possibility of intermetallic phase (sigma and chi) precipitation. Replacing titanium in applications undergoing severe corrosion, like condensers and heat exchanger tubes, is another rationale for the development of these super ferritic steels. Erosion backed by hot-corrosion is a common phenomenon that causes the failure of heat exchangers, boilers and pressure vessels used in coal-fired power generation units. When sodium chloride laded breeze in conjunction with sulfur entrained in fuel deposits on the hot-section component, the degradation of the surface takes place causing severe loss of the material from the inner surface of the generation units. An accelerated attack of oxidation of structural component commonly called as 'Hot Corrosion' occurs by deposition of Na_2SO_4 on a metal surface at high-temperature in range of 700-900℃ [72].

1.8 HOT-CORROSION

In the presence of a reactive environment, metals undergo surface wastage. Such wastage is termed as 'Metallic Corrosion'. The product of such corrosion constitutes of chemical compounds that are close to their original ores. At temperature above 200℃, a significant reaction of metal is seen to occur. However, when exposed to a temperature range of 700-900℃, an accelerated reaction takes place [72]. These reactions involve sulfidation, oxidation or both. Thus, hot corrosion is mainly defined as expedited

oxidation at an elevated temperature that deteriorates the surface under the influence of the film of fused salt deposits. Molten sodium sulfate is the key promoter in causing hot-corrosion. The degree of deterioration is bound by the ionic conducting properties of corrosion products [73]. The thin film of fused salts is present over the surface either in fused state or in solid-state which later turns into liquid on exposure. Thus, the process of hot-corrosion is broadly categorized into two types:

1. **High-temperature hot corrosion:** High temperature (Type-I) hot corrosion (HTHC) normally occurs nearly between 825-950℃ when the condensed phase is in a molten state. The sulfides formation and reactive components depletion in the alloy substrates are the typical characteristics of HTHC. Sulfur is liberated from sodium sulfate which diffuses through the pores, crevice or cracks, on the metal substrate to form sulfides [74]. The corrosion kinetics is dependent on the magnitude and gradient of salt basicity in relation to the local solubility for the oxide scale phases [75]. HTHC produces intense spalling, flaking and massive weight gain in a contentious environment, as observed by several researchers [76–79]**.**
2. **Low-temperature hot corrosion:** Corrosion occurring in the range of 550-750℃, is categorized as Low temperature (Type-II) hot corrosion (LTHC). It occurs much below the melting point of Na_2SO_4 which is 884℃. The product of the reaction is represented by the formation of random pits and depletion of chromium in the alloy substrate [80]. The eutectic Na_2SO_4-MSO_4 (M=Fe, Ni and Co) turns into liquid and causes typical pitting in confined areas [81,82]. The various mechanisms responsible for corrosion have been suggested. But, the salt fluxing mechanism is broadly accepted. The salt fluxing reaction may be acidic

or basic in nature. Species formed in these mechanisms are soluble in water. This dissolution may be either by basic fluxing through anions or by acidic fluxing through cations, thereby, reduces the oxide ions and consequently, the reaction product barrier becomes non-protective [83,84].

1.8.1 Mechanism of Hot-Corrosion

The failure of the protective oxide layer paves a path for the molten salt to penetrate through to the substrate at high-temperature hot corrosion. Metal degradation under hot corrosion consists of two basic stages. The time of transition from one stage to the other is determined by various factors like chemical reaction, erosion, and erosion-corrosion. The two stages discussed below are also represented schematically in Fig. 1.10.

1. **The initiation stage**: implicates oxidization and transfer of metallic atoms from the elements in the alloy to the reducible substance in the deposit. When the molten deposit begins to penetrate the reaction product barrier, small voids are formed. Eventually, the protective barrier becomes ineffective and the propagation stage follows.
2. **The propagation stage:** is generally agreed to follow the salt fluxing mechanism. Due to a shortage of oxide ions during fluxing the reaction product barrier becomes non-protective. This results to form species that are soluble in the molten deposit and gives rise to a phenomenon called 'Fluxing'. Fluxing can be acidic fluxing or basic fluxing.
    a) **Acidic fluxing:** The liquid droplets on the surface has a scarcity of oxide ions and form a non-protective reaction product. The scarcity of oxide ions in Na_2SO_4 can appear because of the presence of some acidic components in the gas. It is caused by the dissociation of oxide ions into the equivalent cation

and O^{2-}. It appears when the activity of O^{2-} is considerably low and leads to severe oxidation reaction. These are self-sustaining since the severity of salt displacement becomes progressively weaker as the reaction proceeds.

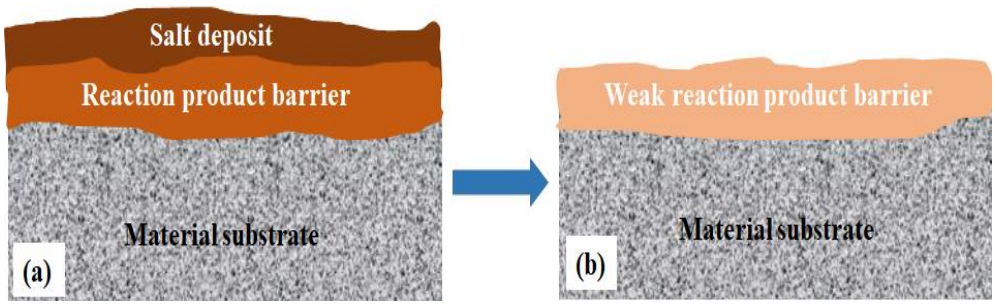

Fig. 1.10: Schematic diagram illustrating the development of hot corrosion during (a) initiation state and (b) propagation stage.

b) **Basic fluxing:** Basic fluxing reaction takes place by combining oxides with O^{2-} forming anions. The sulfur is removed from Na_2SO_4 and consequently oxide scale. They are not self-sustaining since the oxide ions depend on the quantity of deposit present on the surface. Henceforth, a continuous source of Na_2SO_4 is required for this mechanism to proceed.

1.8.2 Hot Corrosion of Stainless Steel

It is well known that hot- corrosion takes place under the influence of high temperature, where the salt mixture coalesces and accelerates the rate of oxide and sulfide formation. With time, products caused by corrosion penetrate through the alloy by diffusion causing deterioration of protective oxides and degradation of materials surface [85,86]. Solid particles impacting on these degraded surfaces, drastically increase the rate of materials loss under the synergistic effect of 'corrosion-erosion' [87].

The resistance of superferritic stainless steel is more than austenitic steels in seawater environment. Their tendency to stress corrosion cracking is fairly low in

chloride-containing solutions. The resistance to localized attack for ferritic steel is calculated using pitting resistance equivalent (PRE).

$$PRE = wt\%Cr + 3.3 \times wt\%Mo + 16 \times wt\%N \quad (1.7)$$

To understand the electrochemical characteristics of stainless steel in acidic, basic or chloride environment, numerous investigations have been done. Findings from these previous investigations suggest that high-temperature corrosion resistance of these materials is low. Nanni et al. [88] considered morphology of scales formed on chromium, manganese and pure iron and studied their corrosion kinetics with Na_2SO_4 deposits in a temperature range of 600-800℃. The material is observed to exhibit accelerated attack which is suggested to be due to low melting liquid sulfate formation. Shih et al. [89] studied the low-temperature hot-corrosion behavior of AISI 304 SS and Fe-Cr alloys when deposited with K_2SO_4-Na_2SO_4 salt mixture. They described the iron dissolution at the interface of oxide melts and re-precipitation of Fe_2O_3 at the melt-gas interface in the form of porous particles. Shi et al. [90] studied the possibility of Na_2SO_4 eutectic melt formation when deposited with Na_2SO_4 at 750℃. It was observed at the site of Cr_2O_3 formation, Na_2SO_4 –Na_2O eutectic was absent for iron-base alloy with high Cr. But, at lower Cr content this eutectic melt was found. This difference may be the outcome of the expedited rate of corrosion. Bornstein et al. [91] proposed a mechanism based on the disintegration of a protective oxide scale in the fused salt i.e. basic fluxing. Goebel et al. [92] stated that the alloys with an acidic component like V or Mo etc., show the occurrence of acidic fluxing with the re-formation of oxides leading to oxidation of Na_2SO_4. Kerby and Wilson [93] investigated the corrosion resistance of certain metals and alloys. They found that stainless steel 440 (with 25% Cr) showed outstanding corrosion resistance to molten V_2O_5. Trinstancho et al. [94] studied hot corrosion on steel

in 80 wt% V_2O_5 + 20 wt % Na_2SO_4 at 540-680°C and recorded the corrosion rate around 7.14 mm/yr. Bala et al. [95] examined the effect of hot-corrosion on Ni-20Cr coated boiler steel (SA516) and recorded a reduction in weight gain to 87.2%. Sidhu et al. [96] suggested that the formation of NiO, Al_2O_3, and Fe_2O_3 on GrA1 boiler steel, when coated with plasma sprayed Ni_3Al, greatly increases the resistance to hot corrosion. The NiO formation reduces the amount of Fe_2O_3 formed by oxidation and thus increases the oxidation resistance of the material. Mangla et al. [97] suggested that HVOF coatings imparted superior properties to resist hot corrosion than plasma sprayed coatings. Trafford and Whittle [98] observed that Na_2SO_4 when present on the surface in the form of fused salt is ineffective to oxidation kinetics. The scale morphology also records any rare change. However, Fe-5Cr exhibits enhanced oxidation initially, with sulfide particles in the alloy substrate. Wang et al. [99] investigated the effect of temperature on the corrosion process of 304SS. The formation and collapse of the protective films is the mode of interaction of stainless steel with chemical and electrochemical kinetics. The interfacial reaction of electrolytic species and their movement within films rely upon the rate constants of these protective films formed. Zahs et al. [100] observed that the corrosion mechanism for Fe, Cr, Ni, and their alloys, for temperature 500°C and above, is active oxidation. Arivazhagan et al. [101] stated that a mixture of NaCl and Na_2SO_4 has a more damaging effect on hot corrosion behavior of stainless steels and superalloys. Shinata et al. [102] highlighted the effect of NaCl induced hot corrosion of stainless steel 304, 316 and 430, and found that corrosion loss increased remarkably for NaCl coated samples. This effect is seen to increase beyond the melting point of NaCl. They also concluded that chromium content in these steels is oxidized preferentially, forming a Cr_2O_3 scale which is non-protective. As a result, the severity of corrosion in the case of high chromium steels are more than lower chromium steels. Sidhu et al.[86] tested the

hot corrosion resistance of Fe-Cr alloy at 800°C in presence of Na_2SO_4 –NaCl salt melt in the open atmosphere. Their finding introduced formation of compact scales on the alloy surface with rare porous oxides. Several workers [89,90,103,104] studied the hot corrosion behaviour of Fe-Cr alloys and commercial iron in the presence of Na_2SO_4 deposits. These materials suffer hot corrosion and formation of complex sulfate eutectic melt is detected. The hot corrosion process for these materials is developed in two-stage. The first stage is the initial stage that records a relatively steep weight gain, involving numerous reactions like oxidation, sulfidation and formation of liquid sulfate eutectics. The second stage is steady-state when both compact and porous corrosion products breed together. The mechanism of Na_2SO_4 induced hot corrosion attack is investigated by many researchers [105,106]. To explain the electrochemical mechanism that involves soluble metal species in hot-corrosion, the dissolution behavior of metal oxide becomes significant. However, the effect of low-temperature hot corrosion of superferritic steels in presence of Na_2SO_4 –NaCl mixture has not been studied. Since the erosion is assisted by corrosion, therefore, a detailed examination of Type 446 stainless steel used as heat exchanger tube materials is carried out to understand their effect on erosion.

1.8.3 Effect of Corrosion on Erosion Behaviour of Steels

Fe-based alloys on exposure to Na_2SO_4–NaCl salt mixture environment undergo a severe problem of hot-corrosion [107,108]. Further operation intensifies the material loss of these corroded surfaces which attributes to excessive occurring solid particles entrained in the fluid. Erosion-corrosion is a process in which both erosion and corrosion operate in synergy. Wood et al. [109] studied erosion-corrosion interaction for marine and offshore materials. They concluded that under the interactive effect of corrosion-erosion, resultant weight loss is greater than an individual simulation of these two factors.

This interaction is termed as a 'synergistic effect'. Here each process is directly influenced by the simultaneous action of the other. Matsumera et al. [110] explained the effect of corrosion on erosion for pure iron. They speculated that removal of the work-hardened layer under high energy impact from the erodent expedited the corrosion attack which in turn enhances the erosion rate of the material. Barik et al. [111] recommended another mechanism for corrosion enhanced erosion by micro-pitting where the number of surface defects increases. Islam et al. [112] carried out cyclic erosion and corrosion test on pipeline steel API X70. They determined both corrosion augmented erosion and erosion augmented corrosion and concluded that the work-hardened layer gets removed under the effect of corrosion. Consequently, the erosion of the corroded surface gets enhanced by exposing these free surfaces. Nava et al. [113] accomplished an erosion-corrosion study to determine the effect of the hardness of the materials. At high temperature, the damage was seen to increase with an increase in hardness, which is credited to the formation of weak protective oxide scales and non-adherent layer. Neville et al. [114] proposed that corrosion enhanced erosion mechanism is due to the selective attack at grain boundaries resulting in increased susceptibility of grain removal by erosion. They also supported the findings by Nava et.al that an increase in hardness showed no effect in increasing the resistance to weight loss for high alloy steels. Dong et al. [115] investigated erosion enhanced corrosion on carbon steel AISI 1020. They stated that on operating in synergism erosion becomes a dominating variable on increasing the flow velocity. Li et al. [116] recommended that localized attack due to particle impact causes disruption in the surface oxide films which enhances crack growth. Burstein et al. [117] suggested that under the effect of the repeated impact of solid particles, detachment of flakes takes place. This detachment of flakes affects the corrosion-erosion of the materials to such an extent that corrosion is almost doubled in the presence of erosion.

Postlethwaite et al. [118] pointed out that erosion being sensitive to the impingement angle, the erosion rate is largely increased under corrosion effect. This is because of the roughness generated over the surfaces due to corrosion. Kim et al. [119] studied the second phase precipitate on erosion-corrosion of 25% Cr duplex stainless steel. They indicated that aging for 30 min was the preliminary treatment for erosion-corrosion, and that the surface damage by mechanical collision during particles impact could be successfully re-passivated. They also suggested that an aging time of 30 min was regarded as boundary aging conditions for stable erosion-corrosion. Laleh et al. [120] on studying the erosion-corrosion behaviour of Selective Laser Melting (SLM) produced 316L stainless steel found that they exhibits high hardness and pitting corrosion resistance. But its corrosion–erosion resistance was significantly low. This may be attributed to weak re-passivation ability associated with pores in the microstructure. Stack et al. [121] examined the effect of oil and water slurry solution on the erosion-corrosion of carbon steel. They also evaluated the velocity and impact angle effect on the erosion-corrosion of carbon steel. The results indicated that the environment containing oil may cater erosion better than water containing the slurry solution. Also, the mechanism of erosion-corrosion changed as a function of impact angle and velocity. Rajahram et al. [122] during investigation of UNS S31603 concluded that increase in velocity and test temperature leads to an increase in the erosion rate due to continuous damage of passive film and metal, caused due to high K.E. of the particle. Also, the interactive effect of sand particle and test temperature showed minimum degradation at lower temperature. Increasing the sand size is seen to produce deep crater and more noticeable lips as compared to smaller particles. Aribo et al. [123] studied the erosion-corrosion behavior of UNS S32304 and UNS S32101 lean duplex stainless steel and found that erosion impact induces work hardening over the surface which eventually

leads to sub-surface microstructure modification. UNS S32304 is seen to have considerable erosion resistance as compared to austenite 304 and duplex UNS S32101. Giourntas et al. [124] experiment demonstrated better resistance to erosion-corrosion of stainless steel compared to medium carbon steel during the assessment of the behavior of different stainless steel in the erosion-corrosion environment. Super-duplex stainless steel performed eminently under low velocity and low sand burdens. They also found that there exists a complex correlation between erosion-corrosion behavior and materials hardness. The tribo-corrosive wear of AISI 316 stainless steel investigated by Zhao et al. [125] concluded that aggregate weight losses of the specimens increased with time. Loss with smaller particles stabilized slowly than larger ones. The easy occurrence of cutting at low impact angles due to dominant shear stress on the metal surface brings about larger weight loss at lower impact angles. Lindgren et al. [126] mentioned that under lower erosion intensity the materials behaved similarly to that in pure erosion. But in case of higher erosion intensity, lean alloy (LDX2101) and 316L suffered from the highest mass loss. This behaviour is better explained by the re-passivation rate. Levy et al. [57] studied the mechanisms and rate of erosion-corrosion in Fe-Cr steels. They determined that erosion of oxide scales formed on the surface was the dominant surface degradation mechanism. The morphology of scales formed on the surface was important than the composition of scales. The presence of Cr_2O_3 in the scales reduced the metal wastage by reducing the formation and removal of scales. Islam et al. [127] assessed the synergistic effect of erosion-corrosion for API X70 pipeline steel and stated that erosion rate of steel increased with increasing particle velocity due to an increase in its kinetic energy. The passive deposits of iron carbonate ($FeCO_3$) ceased from the solution and form a flake-like film on the steel. Thenceforth, exposed stress-free surface for erosion by removing the work hardened layer under the effect of corrosion. The erosion thereby increases the

corrosion and removes the passive film from the surface that subsequently increases the effective surface area. This process of delamination is also accelerated when the solution enters the sub surface cracks. Owen et al. [128] studied erosion corrosion interaction of X-64 carbon steel in aqueous CO_2 environment. They contradicted the statement by Islam et.al. stating that regardless of increase in roughness of the surface the erosion accelerated corrosion was not a significant factor, rather corrosion accelerated erosion was more imposing. The nano-grain layers were through to develop crack due to low cycle fatigue mechanism under erosion impact, with corrosive species accelerating the crack growth. This accelerated crack growth was more significant in erosion-corrosion samples than pure erosion samples. Elemuren et al. [129] investigated the effect of particle concentration on surface roughness of AISI 1018 steel elbow, by carrying out the erosion-corrosion test. Ridges and valleys were formed on the internal wall of the elbow at higher particle concentration. Particle to particle or particle to wall interaction cause degradation of the impacting particle. Strain hardening caused due to impact of abrasive particles leads to an increase in erosion resistance of the material at high particle concentration. Shahali et al. [130] studied corrosion erosion and synergism of Sanicro28 under impact velocity of 4-9 m/s in 3.5% NaCl saline water solution. They recorded an increase in corrosion up to 104 times during erosion as compared with the stagnant condition. With the increase in impact velocity, the corrosion rates increased by around 28 times. This increase in corrosion rate was dependent on the impingement angle, where normal impingement showed more corrosion rate than 40° impingement angle. They also concluded that change of erosion wear due to corrosion was higher and thus synergy rate was highly dependent on the effect of corrosion on erosion. Song et al. [131] investigated the erosion-corrosion behavior of low-alloy steels. They stated that steels with higher tensile strength showed higher erosion-corrosion resistance. Platelets and ring crack

formation due to solid particles striking the sample surface are the mechanisms responsible for their weight loss. The surface is seen to be work-hardened under particle impact and a deformed layer is produced on the surface with lower strength.

Extensive work has been done to study the effect of corrosion on erosion in synergy. However, hot-corrosion which is an important field of study is yet to be explored. The pipelines of the heat exchangers during their operation and maintenance undergo hot corrosion due to salt present in the flowing fluid. The presence of this salt in high-temperature conditions causes hot corrosion, which degrades the material surface and enhances the erosion rate. This study is focussed to study the effect of pre-hot corrosion on the erosion behavior of such materials.

1.8.4 Methods to Mitigate Erosion and Increase Corrosion Resistance of the Materials

High-temperature oxidation and erosion by the impact of fly ash and unburnt carbon particles are a few serious problems that need to be addressed in heat exchangers tubes, power plant boilers, etc. Different protective methods being used to mitigate the wastage arising out of the synergetic effect of erosion and corrosion include:

- Strengthening Mechanism
- Protective coatings for erosion
- Surface treatment for grain refinement

a) Strengthening Mechanism

Like cold working, grain size hardening and solid solution strengthening available for single-phase materials are effective in improving the erosion resistance of eroding materials.

Table. 1.2: Effect of various strengthening mechanism on the room temperature erosion of single-phase material [132].

Mechanism of hardening	Test material	Concluding remark
Annealed pure metal	Pure metals Al, Ni, Cu, Zr	Good correlation between erosion rate and both annealed hardness and melting point
Dislocation strengthening (cold work)	Pure metals Cu, Ni	Erosion resistance was either unaffected or deteriorated with increased cold work
Grain size hardening	304SS, Al, Fe, Fe Cu, Ti	The erosion rate was essentially independent of grain size. Fine-grained Fe was the only exception.
Solid solution strengthening	Cu, Cu-Zn, Cu-Al Ni, Ni-Cr 304SS and 316SS	Solid solution strengthening reduced erosion resistance in Cu-base alloy. Solid solution strengthening improved erosion resistance in Ni-based alloy.

Even in multiphase alloys, strengthening mechanism results in substantial improvement in materials strength but the erosion resistance changes only marginally. In the case of intermetallic, erosion rate is seen to be lower than the base material but the erosion rates of various intermetallics are comparable in spite of their varying crystal structure and melting point. Table 1.2 shows a wide variety of quenched and tempered steel that has been studied to characterize their erosion behavior. McCabe et al. [133] concluded that spheroidized steel exhibited a minimum erosion rate while martensite

microstructure showed maximum erosion rate. Pearlite and tempered martensite have intermediate erosion rates.

b) Protective Coatings for Erosion

Although different types of coating techniques are available, however, from economic as well as availability point of view the methods shown in Fig. 1.11 are currently used:

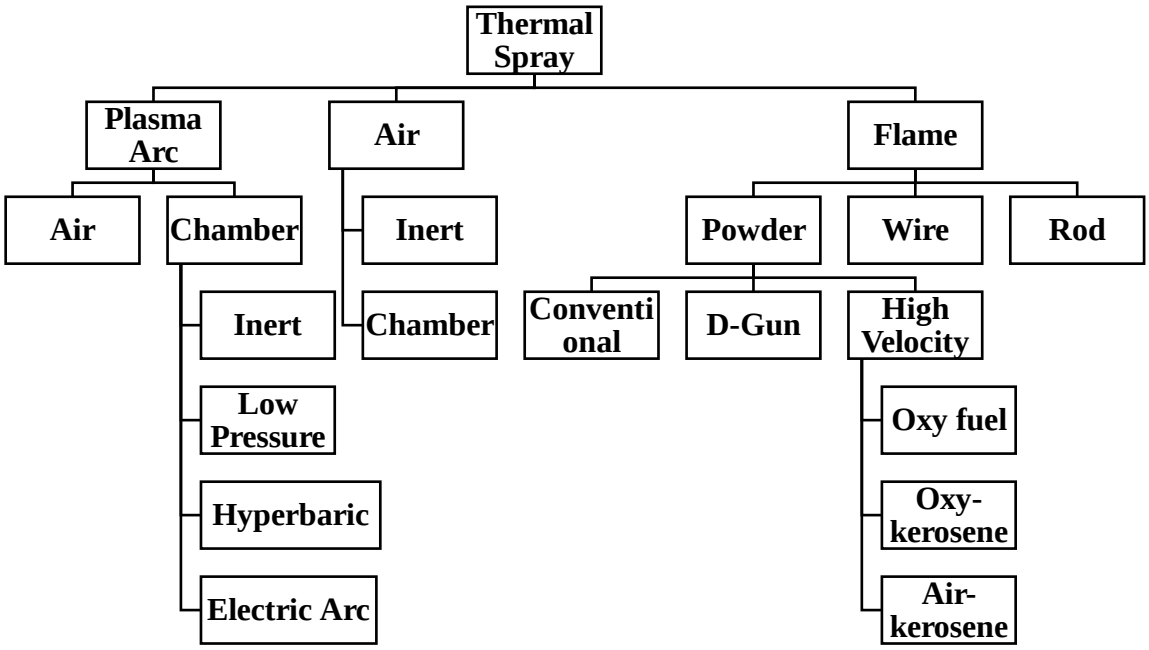

Fig. 1.11: Classification of the thermal spray coating process [134].

c) Surface Treatments for Grain Refinement

Nanostructured materials possess superior mechanical and physical properties, improved corrosion resistance, and higher wear resistance. The nanostructured surface is synthesized using two complementary approaches

- **"Top-down" approach:** the existing coarse-grained materials are processed to achieve grain refinement and nanostructure, involving large plastic deformation, in which materials are subjected to large

plastic deformation**.**

- **"Bottom-up" approach**: in which nanostructured materials are assembled from individual atoms or from nanoparticles.

Numerous techniques are developed to form surface nanostructure. Some of them are listed as are ultrasonic shot peening (USSP)/surface mechanical attrition treatment (SMAT), laser shock peening, hammer peening, surface rolling, and high-speed drilling. These surface treatments introduce compressive residual stress along with refining the microstructure in the surface region of the components. Ultrasonic shot peening (USSP) induces compressive residual stress to larger depth and also refines the microstructure of the surface region even up to nanoscale.

1.9 ULTRASONIC SHOT PEENING (USSP)

Apart from various discussed techniques, surface modification is the most promising route to enhance the erosion-corrosion behavior of materials substrate. Several processes of surface modifications and microstructure development, like, severe plastic deformation, surface coatings, ball milling, shot peening, friction stir processing, LSP and USSP takes the advantage to intensify the surface properties of the structural component [135–137]. In general, plastic deformation techniques have proved to be instrumental in modifying the corrosion resistance of the metallic material. USSP is a relatively new technique of grain refinement that significantly improves the mechanical properties of metallic materials by inducing compressive residual stress through ball impact over the surface and brings no change to their chemical composition [138,139]. Fig. 1.12 shows a schematic representation of the USSP process.

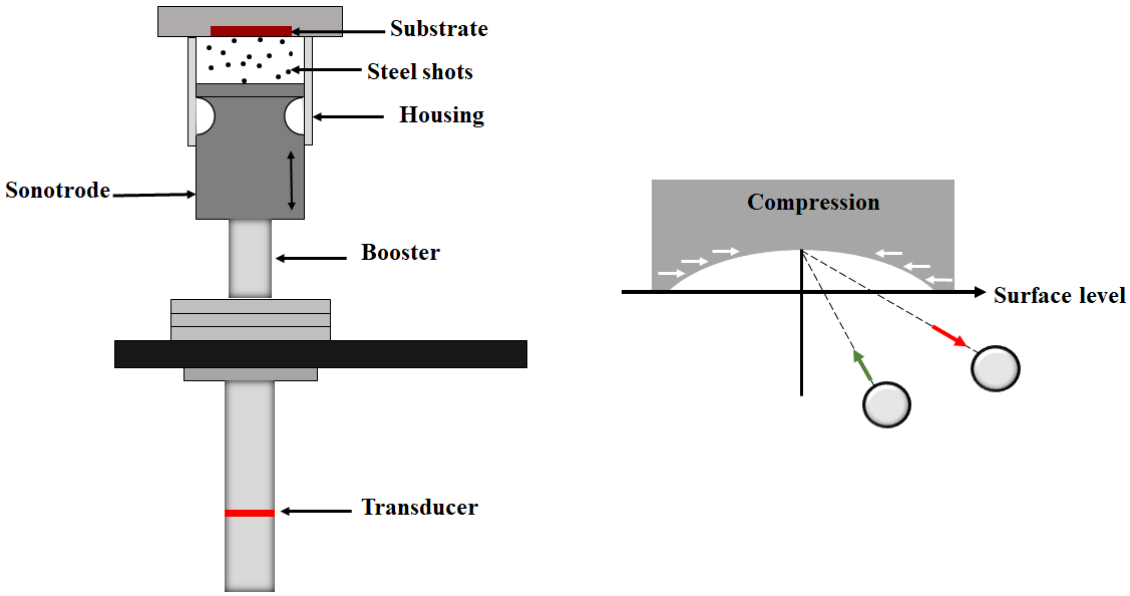

Fig. 1.12: Schematic showing the principle of ultrasonic shot peening.

The impacting balls in Fig. 1.12 act as a hammer creating indentation or semi-sphere, thereby increasing the hardness of the surface. USSP generates grain refinement along with other defects which provide a short-circuit path for the diffusion of beneficial solute atoms at the free surface and create a protective oxide layer [140,141]. The compressive residual stresses developed in the surface and sub-surface regions together with grain refinement increase the corrosion resistance and thus, the life span of the component [142,143]. Under the effect of USSP treatment, the rapid diffusion of chromium ions along grain boundaries as compared to through grain themselves improves the corrosion and oxidation properties of ferritic steel [144,145]. The corrosion nature of materials with modification in superficial properties is a promising area to explore [146,147]. The corrosion rate increases two folds in the presence of erosion, which is responsible for generating flakes on the surface under the repeated impact of the particle [148]. Hot corrosion resistance is improved by USSP [149,150]**.** The effect of USSP on hot

corrosion-erosion behavior of high chromium ferritic steel is hardly investigated and reported.

1.10 SCOPE OF THE PRESENT WORK

Several operational difficulties are encountered with heat exchanger units leading to damage or failures and consequently forced outages. Among these, mechanical damage due to erosion is a complex phenomenon. This component suffers from combined hot corrosion and high-temperature erosion in an actual service environment. The presence of salt particulates in the ingested fluid leads to the deposition of a highly damaging compound of sodium sulfate on the surface of heat exchanger tubes, leading to expedited hot corrosion. This results in roughening of surface which causes severe damage to the component under high energy erosion impact and results in premature failure of the tubes.

So far, the researchers have only focused on mechanical damaging of the tubes that occur due to tube fretting or fatigue cracking. Very limited literature is available on erosion-corrosion life estimation based on actual operating conditions. Therefore, it is important to study the hot corrosion behavior in air and salt environment to assess the effect of high-temperature erosion-corrosion on tube damage. Following an exhaustive survey of candidate material and a review of their strength and weakness, it is foresighted that ferritic steel would prove to be a potential material for heat exchanger tubes. An important group of stainless steel, which is ferritic in structure is an iron-chromium alloy with 17-30 wt% chromium. These steels, particularly at higher chromium levels, have excellent corrosion resistance, as equal as 18-8 Cr-Ni steel, in many environments. When annealed, these are completely free from stress corrosion and are therefore a substitute for the austenitic stainless steel. The response of material towards high-temperature

erosion when working with temperature in the range of 200°C to 800°C restrict the investigators to observe the behavior in the specified temperature zone.

The present work is aimed to investigate the behavior and performance against the erosion of Type 446 stainless steel steel under actual operating conditions. Erosion tests must be conducted to evaluate the behavior of Type 446 stainless steel at a higher temperature. Response Surface Methodology (RSM) can be used to optimize the levels of these variables to attain the best system performance. To approximate a response function to experimental data, a quadratic response surface, i.e., Central Composite Rotatable Design (CCRD) will be helpful in the present study. Advances in computing power have enabled the application of ANN in providing non-linear modeling for response surfaces and optimization. Therefore, ANN offers an alternative to the polynomial regression method as a modeling tool.

The scope of the present investigation includes a systematic investigation on the influence of hot-corrosion enhanced solid particle erosion behavior of Type 446 stainless steel used in heat exchangers. The test specimens were hot-corroded using NaCl and Na_2SO_4 deposits by the spray deposition technique. Surface nanostructuring is considered to be helpful in reducing the corrosive attack, therefore, an attempt is made to study the effect of surface nanostructuring by ultrasonic shot peening (USSP) on hot corrosion resistance of Type 446 stainless steel in the above-mentioned test environments. The problems arising due to the synergistic effect of corrosion enhanced erosion are severe and their complexity is not thoroughly understood. Therefore, the pre-hot-corroded samples were exposed to erosion, to mimic the corrosion enhanced erosion behavior. Both corrosion kinetics evolution and morphological development are

investigated by means of weight gain measurements, metallographic examination, and identification of the corrosion products.

1.11 MOTIVATION OF STUDY

Metallic substrate when exposed to high temperatures suffers hot-corrosion and development of thick scales (oxides, sulfides, etc.) leading to the synergistic interaction between SPE and corrosion. The synergetic effect of erosion-corrosion needs appreciable attention to scale down material degradation in several applications including Coal gasification, steam turbines, jet turbines, water walls, and heat exchanger tubes. An extensive survey on erosion-corrosion in high temperature and high-pressure conditions has been carried out and found that heat exchanger, piping and valves as the most affected component. Iron and Nickel and their oxides are thermodynamically unstable in sulfidizing atmosphere resulting in the formation of non-protective sulfides that tend to become molten and accelerate attack at the necessary operating temperatures. Chromium is the most beneficial alloying element in this regard.

The present work is related to the study of high chromium ferritic steel at high-temperature erosion-corrosion behavior when exposed to a corrosive atmosphere containing chlorine and sulfur. As discussed above, chromium being a beneficial element, the selected material Type 446 stainless steel may offer to substitute the existing material in heat exchanger applications. Heat exchanger forms a vital part of many processes and has always been of great industrial importance. The requirement of heat exchangers demands steady materials with improved efficiency and cost-effectiveness which can meet the environmental need at the same time. Mechanical damage caused due to tube fretting and wear, fatigue cracking and erosion-corrosion cause operational difficulty. They may necessitate repair at a high cost and forced premature replacement

of the component. Based upon principal selection criteria, the variety of materials chosen are ferritic steel, 2.25Cr-1Mo, 9Cr-1Mo and austenitic stainless steel (304, 316, 321). Among these, ferritic steel is the preferred choice since it exhibits increased protection to stress corrosion cracking after annealing.

1.12 OBJECTIVES OF THE PRESENT INVESTIGATION

The objectives of the present investigation are to study the effect of the following:

- High-temperature erosion behavior of superferritic Type 446 stainless steel under the variable angle of impact at room temperature and 200, 350, 550 and 650°C, using impact velocity of 100 m/s at both oblique impacts and normal impacts. To understand the different erosion processes.
- Optimization of variables responsible for the loss of materials using Design of Experiment (DOE) and Artificial Neural Network (ANN). The variable had a range of temperatures from 350 to 750°C, velocity varying from 40 to 100 m/s and impact angle changes from 30º to 90º.
- Pre-hot corrosion by two salt mixture (75 wt.% Na_2SO_4 + 25 wt.% NaCl) on high-temperature solid particle erosion behavior of the superferritic Type 446 stainless steel at 550, 650 and 750°C, to predict the response of a material to the erosive environment.
- Modification of surface using ultrasonic shot peening (USSP), to develop compressive residual stress on the surface and enhance the corrosion – erosion resistance of the material, to develop an erosion-resistant material.